Exp Fluids (2009) 46:683–692
DOI 10.1007/s00348-008-0594-1

RESEARCH ARTICLE

Velocity profiles and interface instability in a two-phase fluid: investigations using ultrasonic velocity profiler

A. Amini · G. De Cesare · A. J. Schleiss

Received: 23 October 2007 / Revised: 12 September 2008 / Accepted: 30 October 2008 / Published online: 2 December 2008

Abstract In the present study the velocity profiles and the instability at the interface of a two phase water-oil fluid were investigated. The main aim of the research project was to investigate the instability mechanisms that can cause the failure of an oil spill barrier. Such mechanisms have been studied before for a vast variety of conditions (Wicks in Fluid dynamics of floating oil containment by mechanical barriers in the presence of water currents. In: Conference on prevention and control of oil spills, pp 55–106, 1969; Fannelop in Appl Ocean Res 5(2):80–92, 1983; Lee and Kang in Spill Sci Technol Bull 4(4):257–266, 1997; Fang and Johnston in J Waterway Port Coast Ocean Eng ASCE 127(4):234–239, 2001; among others). Although the velocity field in the region behind the barrier can influence the failure significantly, it had not been measured and analyzed precisely. In the present study the velocity profiles in the vicinity of different barriers were studied. To undertake the experiments, an oil layer was contained over the surface of flowing water by means of a barrier in a laboratory flume. The ultrasonic velocity profiler method was used to measure velocity profiles in each phase and to detect the oil–water interface. The effect of the barrier geometry on velocity profiles was studied. It was determined that the contained oil slick, although similar to a gravity current, can not be considered as a gravity current. The oil–water interface, derived from ultrasonic echo, was used to find the velocity profile in each fluid. Finally it was shown that the fluctuations at the rearward side of the oil slick head are due to Kelvin–Helmholtz instabilities.

A. Amini (✉) · G. De Cesare · A. J. Schleiss
Ecole Polytechnique Fédérale de Lausanne (EPFL), ENAC, ICARE, LCH, Station 18, 1015 Lausanne, Switzerland
e-mail: azin.amini@epfl.ch; aamini@stanford.edu

G. De Cesare
e-mail: giovanni.decesare@epfl.ch

A. J. Schleiss
e-mail: anton.schleiss@epfl.ch

1 Introduction

The main aim of the present research was to investigate the efficiency of flexible oil spill barriers in containment of slicks caused by marine accidents in the open seas (Amini 2007). For this purpose, two-dimensional experiments were carried out in a laboratory flume with different barrier depths. To achieve a better understanding of the response of the barrier at different flow velocities, it was important to measure the velocity profiles in each fluid and to study the instability at the oil–water interface for different barrier geometries.

Velocity measurements are used in various fields of research. In hydraulics, a variety of velocity measurement methods exist, e.g. Pitot-tube, electromagnetic field, laser technology (LDA), particle imaging velocimetry (PIV), and ultrasonic velocity profiling (UVP). The UVP measurement technique was developed by Takeda (1995) to measure an instantaneous velocity profile of liquid flows, using Doppler shifted frequency in echoes reflected by small particles flowing with the liquid. This method was used to study the flow mapping of turbidity currents in a laboratory flume by De Cesare and Schleiss (1999) and showed the capability of such an instrument to detect the interface between the turbidity current and the ambient water.

In the present study, a non-intrusive velocity measurement method was required i.e. one that would not disturb the flow. The selected method was thus UVP.

The applicability of the UVP method to study flow with large fluctuations in both the velocity and orientation of gas–liquid interface was confirmed by Nakamura et al. (1996, 1998). Recently the capability of this method to detect the interface of a two-phase flow was verified by Amini et al. (2006).

2 Experimental facilities and measurement device

Experiments were conducted in a 6.5-m long, 1.2-m deep, and 0.12-m wide laboratory flume, where the water level was fixed at 0.9 m. A barrier was placed across a flume containing an oil layer over s water surface (Fig. 1). Experiments were carried out for rigid and flexible barriers with different drafts.

Experimental conditions are presented in Table 1. Measurements were done for each experiment once before adding the oil, and again in presence of oil. The added oil volume was 2.4 dm^3, giving 20 dm^3/m per unit width of the barrier. For each test, after establishing a certain mean flow velocity in the flume, rapeseed oil was poured over the water surface upstream of the barrier. The rapeseed oil has a density of 0.91 g/cm^3, and a viscosity of 88.8 cSt. The interfacial tension of rapeseed oil and water is 30 mN/m. For such an oil with relatively low viscosity, the so-called entrainment failure can cause the oil to be transferred underneath the barrier. Entrainment failure occurs when a high relative oil–water velocity may cause interfacial waves and oil droplets to be entrained from the oil–water interface and pass beneath the barrier (Wicks 1969; Fannelop 1983; Fang and Johnston 2001).

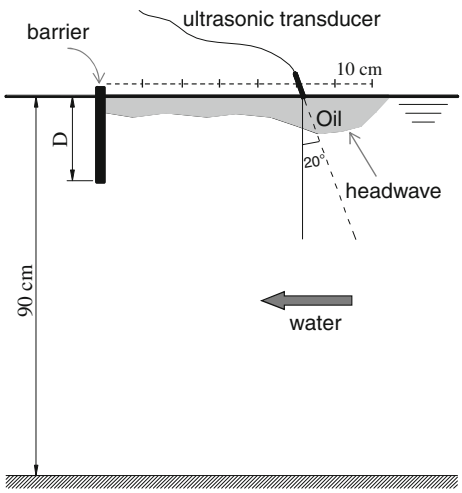

Fig. 1 Schematic drawing of the experimental setup; water is flowing from right to left; oil slick is contained upstream of the barrier; distance between two measuring point is 10 cm; *D* is the draft of the barrier

Table 1 Experimental conditions

Parameters	Value
Water depth (m)	0.9
Barrier draft (m)	0.1, 0.2
Mean water flow velocity (m/s)	0.15, 0.20, 0.25
Contained oil volume (dm^3/m)	20

Table 2 Main parameters of UVP measurement

Parameter	Value
Number of channels	600
Number of profiles	512
Sampling period (ms)	100
Window start (mm)	3.7
Window end (mm)	446.96
Channel distance (mm)	0.74
Channel width (mm)	0.74
Frequency (Hz)	2

As illustrated in Fig. 1, the ultrasonic transducer was installed on top of the oil, and it was inclined at an angle of 20° in the upstream direction. The flow was not disturbed by the transducer as it just touched the oil surface. The main UVP measurement parameters are listed in Table 2. The UVP technique requies a reflecting echo, which was provided by air bubbles using a porous pipe at the inlet of the flume upstream of the measurement zone.

Measurements were taken along the oil slick at every 10 cm as it is illustrated in Fig. 1. The transducer was displaced to the measurement point and after running a measure it was moved to the next point. Velocity was measured over 40 cm depth (inclined distance of about 45 cm) from the water surface.

3 General observations and results

Measurements were carried out in the central plane of the flume. The velocity field was previously detected by the LSPIV method (Amini et al. 2008) which showed that the assumption of one dimensional flow is plausible upstream of the barrier. The measurement angle was then corrected on the flow direction. The corrected velocity profile at each measuring point, averaged over the measuring time (51 s), represents the horizontal component of flow velocity. For experiments with oil, since the interface was oscillating in the vertical direction, the averaging is less accurate in the vicinity of the oil–water interface.

The laboratory effects and potential measurement errors must also be considered. The velocity magnitude was

calculated based on the speed of sound in water (c_w = 1,483 m/s). In principle, the velocity in oil should be modified by using the speed of sound in oil, c_o = 1,445 m/s. However, since the difference is not considerable, it was neglected. As the sound velocity in water and oil are close, the total reflection angle is relatively high (76°) with respect to a line normal to the interface. The inclination angle here was 20°. Thus, reflection did not occur at the interface, except in the case of very steep interfacial waves.

At low flow velocities, the measured velocity profiles are disturbed due to the ultrasonic reflection at the well-defined oil–water interface. Figure 2a illustrates this phenomenon for an experiment at mean flow velocity of 15 cm/s. As it is shown, the reflection of the ultrasonic pulse leads to a multiple echo in the oil layer. At lower velocities, where the oil surface is not yet fluctuating, the interface works as a mirror and this effect is amplified and noticeably influences the measured profiles (Fig. 2b). This phenomenon was previously described by Willemetz (1996). To achieve more accurate results a modified profile, as shown in Fig. 2c, should be considered. To modify the results a logarithmic curve was fit to points with maximum local velocity (Fig. 2c). The variation of the mean flow velocity with depth below the oil–water interface can be assumed to be logarithmic and can be derived using Eq. 1 (Schlichting and Gersten 1999).

$$u = \frac{1}{k}\ln\left(\frac{z}{z_0}\right) \quad (1)$$

where u is the velocity at distance z below the oil–water interface divided by friction velocity, u^*. k is the von Karman constant $k = 0.41$. In absence of an exact value of z_0, it can be taken as a devision of the depth of the velocity profile below the interface, z_d. The equation was imposed to points with maximum local velocity and the deviation was minimized changing z_0 keeping k unchanged. The best fit curve corresponds to $z_0 = 10^{-4}$ times the depth z_d, i.e. a very smooth interface.

At higher velocities the interface is no more stable and cannot act as a mirror; therefore, no multiple echo happens.

The superposed velocity vectors and velocity fields for rigid barriers with 10 and 20 cm draft and at three different flow velocities are presented in Figs. 3 and 4. Figure 5 shows the results for a flexible barrier with 20 cm draft. Velocities are compared for the same experimental conditions with and without oil. The approximate oil slick thickness was measured visually during the experiments and it is superposed on the figures showing results of experiments with oil.

As it can be seen, the presence of oil over the water surface does not influence the velocity field considerably. However, the influence of the oil layer on the flow pattern becomes more significant at higher flow velocities. A different velocity field results in a different force on the barrier, which should be considered in design of oil barriers.

Near the barrier region, where the vertical velocity increases, the horizontal velocity diminishes. The measured velocity close to the barrier is smaller in the case of a deeper barrier comparing to a shorter one, and for a rigid barrier comparing to a flexible one. This reduction was also seen to be more significant in case of experiments with oil.

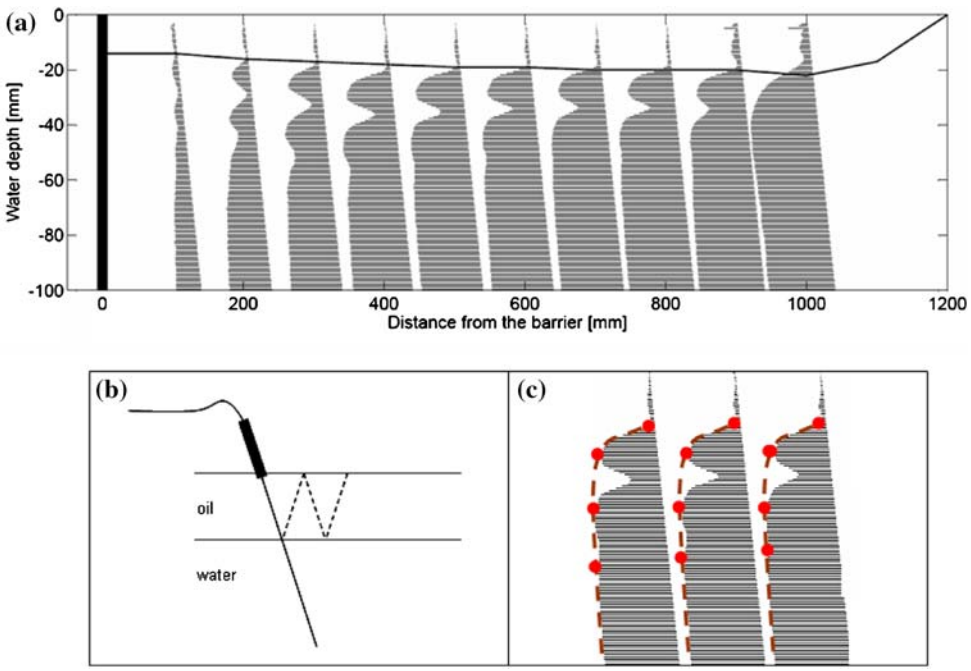

Fig. 2 Laboratory effects on velocity profiles due to multiple echo: **a** disturbed velocity profiles by effect of multiple echo for mean flow velocity of 15 cm/s; **b** schematic explanation for the problem; **c** modified profiles in dashed line

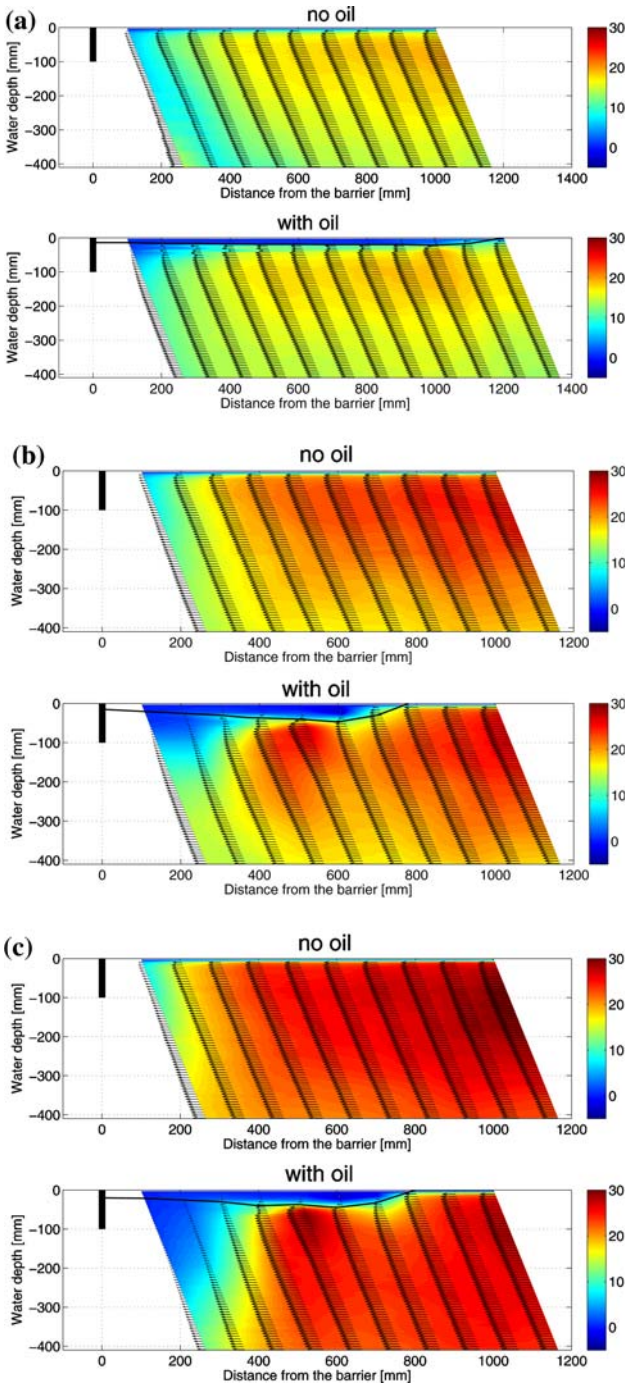

Fig. 3 Horizontal velocity vectors and velocity field for a rigid barrier with 10 cm draft and mean flow velocity of **a** 15 cm/s; **b** 20 cm/s; **c** 25 cm/s

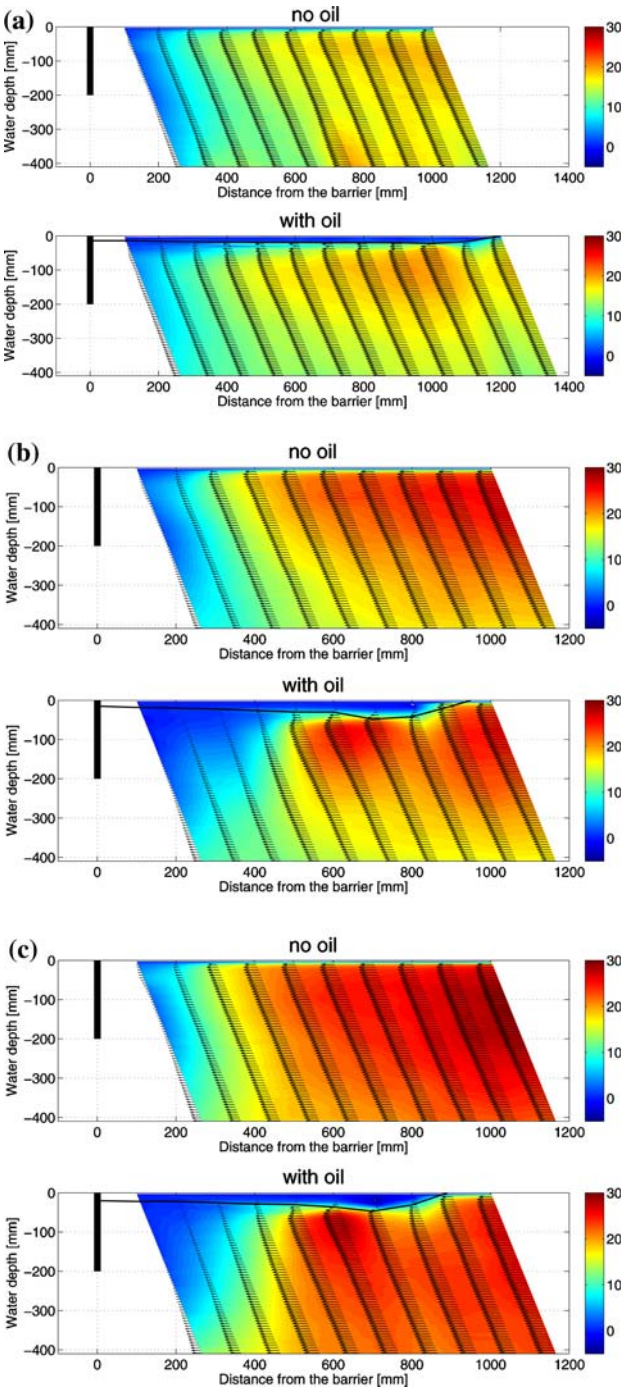

Fig. 4 Horizontal velocity vectors and velocity field for a rigid barrier with 20 cm draft and mean flow velocity of **a** 15 cm/s; **b** 20 cm/s; **c** 25 cm/s

The reason can be explained due to the headwave effect, which causes the streamlines to detach from the surface earlier.

The presence of a headwave causes an obstacle for the flow and makes the velocity vectors to decline. As such, the flow diverts locally from a horizontal pattern and becomes locally two-dimensional. That leads to a reduced measured velocity by UVP probes that can measure the projection of velocity vectors on the measuring axe (20°).

The maximum value of the horizontal velocity occurs after the headwave. This phenomenon is quite similar to the case of a gravity current in a sheared ambient flow and will be discussed in detail in Sect. 4.

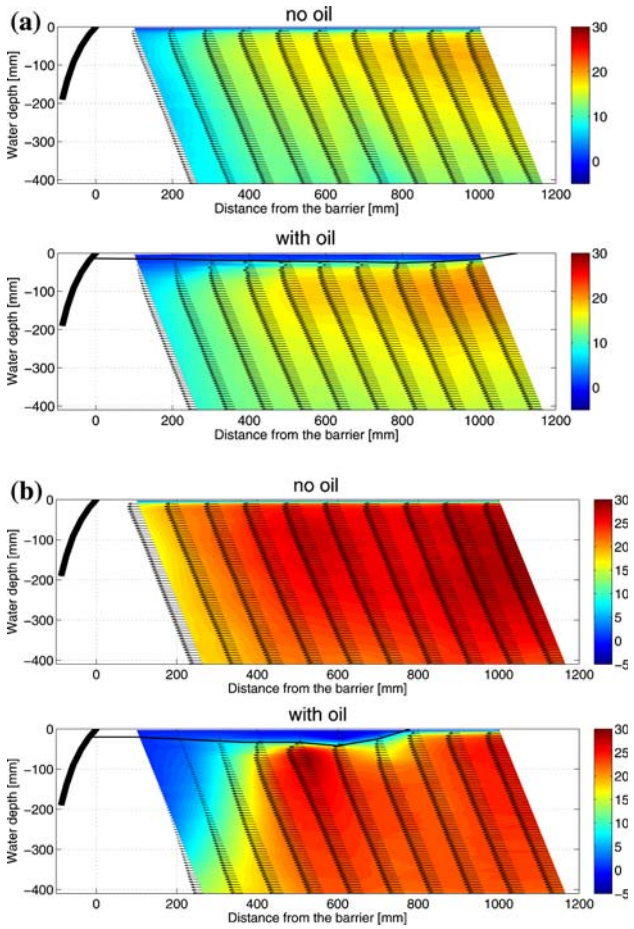

Fig. 5 Horizontal velocity vectors and velocity field for a flexible barrier with 20 cm draft and mean flow velocity of **a** 15 cm/s; **b** 25 cm/s

The velocity field in the vicinity of the barrier is influenced by the barrier draft. However, this influence is limited to a distance of about once the barrier draft. At higher velocities the influence of the barrier draft becomes more significant.

Considering the results of experiments with different conditions, several zones in Figs. 3, 4 and 5 were studied. Figure 6 shows the measured velocity at different distances from the barrier in different conditions, and at three different depths for a mean flow velocity of 15 cm/s. The left column in the figure shows the results of experiments without oil, and the right column shows the obtained results for experiments with oil. It can be seen that for experiments with 10 cm draft (first row), the presence of oil has no significant influence on the velocity value. On the other hand, for barriers with 20 cm draft, as also shown in Figs. 3 and 4, velocities are different for tests with and without oil. Figure also shows that at points close to the barrier, the velocity is highly influenced by the barrier draft. Comparing the results of rigid barriers shows that in the near barrier region velocities are more than two times higher for a barrier with 10 cm draft than for a barrier with 20 cm draft.

4 Characteristics of a contained slick: analogy and difference with gravity currents

At upstream end of the contained slick the oil layer is thicker and the oil–water interface is more unstable when compared to the other parts of the slick. This part of the slick with local thickening is known as its "headwave". Many investigators, including (Wicks 1969) and more recently (Simpson 1997), have noticed the analogy between the headwave region of a contained oil slick and the frontal part of a gravity current turned upside down. However, Milgram and Van Houten (1978) have shown that the headwave in contained oil slicks substantially differs from that of gravity currents. They implied that there are two important differences between the oil layer and the gravity current: the existence of a free surface above the oil, and a shear stress at the oil–water interface. These characteristics are the subject of detailed discussions in this section. The characteristics of gravity currents presented by several research studies are explained first. Then a comparison between gravity currents with the contained slick headwave is made.

In an early study, Von Karman (1940) proposed a theoretical model for the head of density currents in which the angle between the bottom and the front interface is about 60°. Based on this model, Benjamin (1968) studied the phenomenon and postulated that headwave rises to a little over twice the mean height of the interface, and on the rearward side there is a highly turbulent zone suggestive of some kind of wave breaking process. In the model, he proposed a nose-shaped structure at the front of the head. Simpson (1972) studied the effect of the lower boundary layer and stipulated that within the head the lower boundary controls the detailed form of the structure. An empirical dependence of nose height on Reynolds number was also established.

Britter and Simpson (1978) explored the mixing of the gravity current and ambient flow, suggesting that this mixing occurs through Kelvin–Helmholtz instability. Later, Simpson and Britter (1979) described the motion behind the head of a gravity current as a complex three dimensional flow which is a result of gravitational and shear instabilities at the head. To verify the effect of the velocity profile (sheared or uniform) on gravity currents, Xu (1992) developed a two-phase model, and confirmed that the depth of the density current and the vertically averaged frontal slope increase with the positive shear. He also postulated that the turbulence at the head is due to a hydraulic jump.

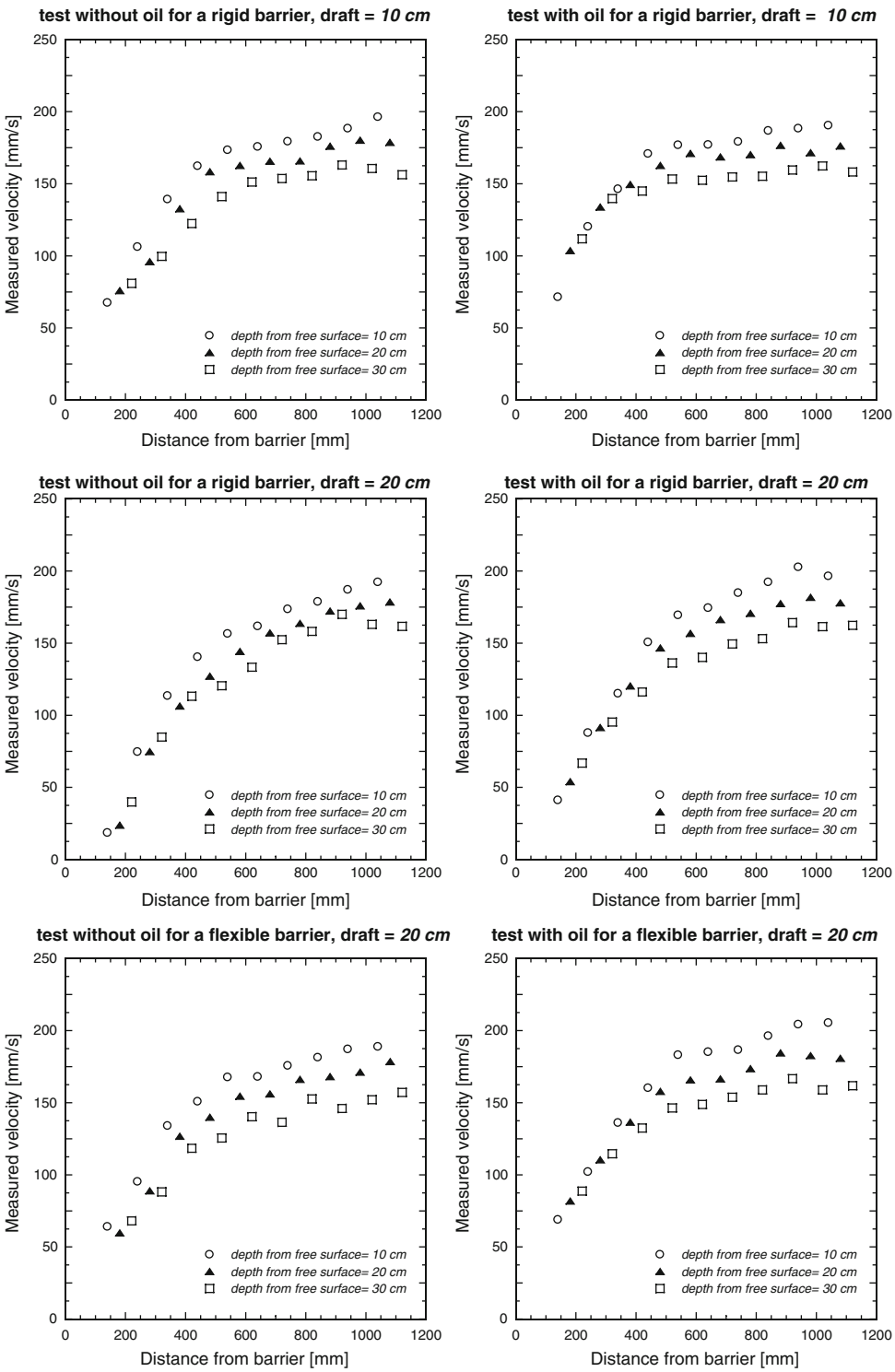

Fig. 6 Measured velocity at different distances from the barrier at mean flow velocity of 15 cm/s; *left column* shows results for experiments without oil; *right column* shows results of experiments with oil

Contrary to the suggestion of Von Karman (1940), Xu and Moncrieff (1994) implied that when the inflow shear is sufficiently strong, the interface will become locally steeper than 60° at middepth of the density current.

Recently, Shin et al. (2004) investigated the gravity currents produced by lock exchange. They studied a surface gravity current with fresh water as the less dense fluid and a solution of sodium chloride as the denser fluid. The gravity current had a deep head with billows, and mixing occurred at the rearward side. Immediately at the rear of the head the current was shallower than both the head and the current further behind. The mixing region was confined to within one or two head heights of the front, after which the edge of the current was stable and there was no

appreciable mixing. They proposed a front/headwave Froude number of 1 rather than the previously accepted value of $\sqrt{2}$. This number is expressed as:

$$F_{\mathrm{h}} = \frac{U_c}{\sqrt{g\,\Delta\,t_h}} \tag{2}$$

where U_c is the gravity current velocity (or oil internal velocity in the present study), g is the gravity acceleration, Δ is the relative oil density, which is expressed as $(\rho_w - \rho_o)/\rho_w$, and t_h is the thickness of headwave.

Apart from geometrical analogy, a common feature in oil slicks and gravity currents is the fact that the horizontal velocity component reaches its maximum value after the headwave or current front. Figure 7a illustrates a gravity current with a shear inflow presented by Xu (1992). In the model the energy loss and generation of negative vorticity that can take place due to dissipation by breaking of the interface and turbulence generation was taken into account in the formulations for the outflow. In the present study with oil, similar to the Xu model, the ambient flow is sheared (Fig. 7b). Hence, the same zone of maximum velocity was measured at the rearward side of the headwave.

It was shown by Amini (2007) that for an oil slick, the headwave is 1.5–2.5 times thicker than the mean oil layer thickness in other parts of the slick. This is similar to the results reported by Benjamin (1968) saying that thickness of the front of a gravity current is a little more than twice the mean height of the interface.

The dissimilarities between the slick headwave and the frontal zone of a gravity current are listed below:

- The angle between the bottom and front interface is 60° or more in the case of a gravity current, but in the case of an oil slick, the measured angle was about 45°. This angle is shown in Fig. 8. In the figure at the upstream end of the slick two oil colors can be seen. The lighter color is due to adhesion of oil on the lateral walls as shown in the plan view. The area with a darker yellow color corresponds to the central plane of the flow, where the oil shape is not influenced by the effect of lateral walls.
- A gravity current has a nose at its front, which is not the case in an oil slick. This can be explained due to effect of lower boundary friction for a gravity current that does not exist for an oil slick with free surface. However, in the presence of wind or surface contamination, a nose could possibly form at the headwave of an oil slick.
- The front Froude number is proposed to be 1 to $\sqrt{2}$ for a gravity current, which means that the head is super-critical, and the mixing at the rearward side is due to a hydraulic jump. However the headwave Froude number is of a lower order for oil slick (0.15–0.25), and the head is sub-critical. The breaking interfacial waves are due to Kelvin–Helmholtz instability, as it will be discussed in Sect. 6.
- The flow in a contained slick is laminar ($Re \approx 500$), contrary to gravity currents which are high Re number turbulent flows.
- In gravity currents, billows are formed on the rearward side of the head, while in an oil headwave they were seen forming at frontward side.

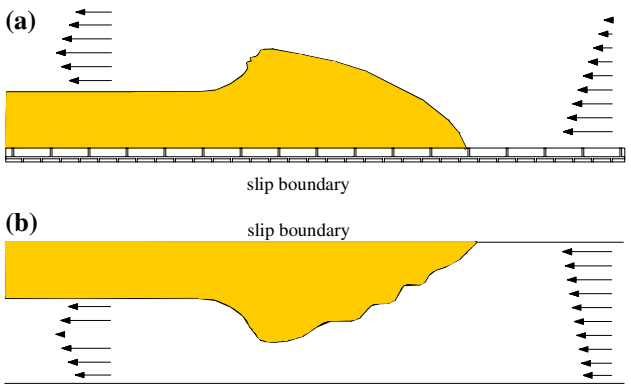

Fig. 7 Comparison of head in gravity currents and observed headwave in the present study: **a** model presented by Xu (1992) for a gravity current in shear ambient flow; **b** observed headwave of oil slick with fluctuations in the front side

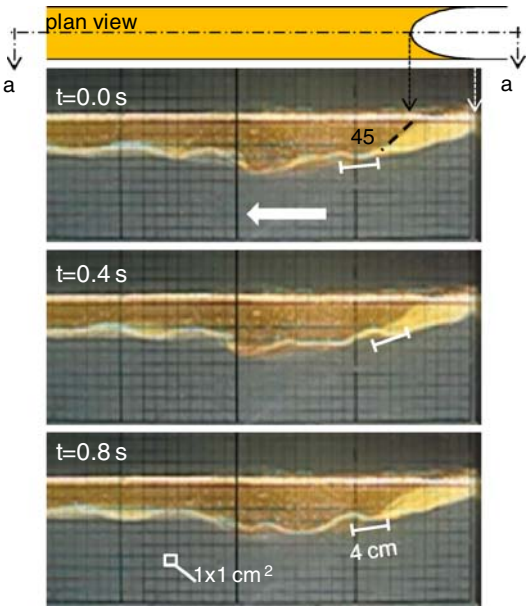

Fig. 8 Interfacial waves forming at frontward side of the oil slick headwave, sequence of pictures is 0.4 s; grid size is 1 x 1 cm^2; water is flowing from right to left with a mean flow velocity of 15 cm/s; barrier draft is 10 cm; *a–a* line shows the measurement section; wave length was observed to be about 4 cm; the "light yellow" zone of the headwave is due to wall adhesion of the oil

- Oil and water form an inmiscible interface that causes separated phases. In gravity currents the interface is miscible and the fluids can mix together more easy making a mixture at rearward side of the head.

As a result, it can be concluded that even though there are similarities between gravity currents and headwave of oil slicks, the phenomena are quite different.

5 Interface detection and velocity profiles in oil and water layers

Investigating the interfacial fluctuations and detecting the position of the oil–water interface require precise measurements. UVP measurements were for the first time applied to detect the oil–water interface by Amini et al. (2006). The hypothesis that the ultrasonic echo has its maximum value at the oil–water interface was verified by studying the oscillations at the rearward side of the slick headwave, where interfacial waves are more regular. For that purpose the power spectra were studied.

Power spectra show distribution of liquid fluctuation energy of one channel as a function of frequency (Met-Flow 2002). For power spectrum calculations, complex velocity $V(f)$ as a function of frequency is first calculated by Fast Fourier Transform (FFT) of velocity time series $v(t)$:

$$V(f) = \mathrm{FFT}(v(t) \times w(t)) \tag{3}$$

where $w(t)$ is the windowing function, assumed to be a rectangular windowing function, i.e. $w(t) = 1$, since no remarkable difference in the result is observed for alternative windowing functions.

From complex velocity image in frequency domain, the power spectrum is then calculated:

$$P(f) = (V(f))^2 \tag{4}$$

By definition, the power spectrum gives the portion of signal power falling within a certain frequency, and its peak corresponds to the most commonly occurring frequency (Lyons 2004).

Figure 9 illustrates an example of the power spectrum in the vicinity of an observed interfacial point, with its frequency peak at 2.62 Hz. In this case the location of interface was observed to vary between 3.2 and 4.8 cm from the UVP transducer. Hence, a spatial average of the power spectrum over the region where the oscillation was observed was taken. This averaging cancels the random noise in the spectrum and a clearer peak structure can be obtained. The average value for 21 spectra, corresponding to points located in the oscillation amplitude, was 2.53 Hz, i.e. the period of oscillations was about 0.4 s. Sequential

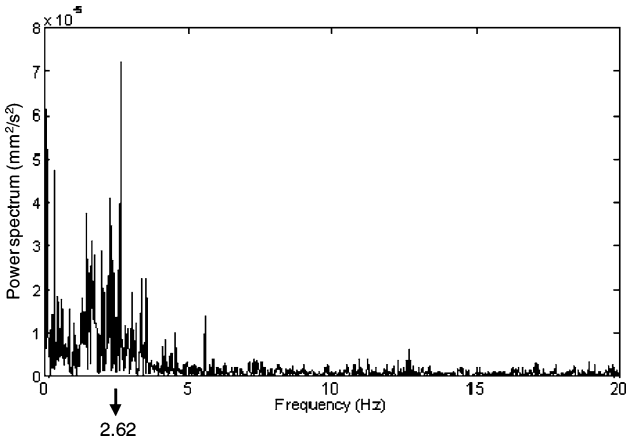

Fig. 9 Power spectrum in the vicinity of the observed interface

photos of the same experiment showed a period of about 0.4 s for interfacial oscillations at the considered point. It confirms that the maximum echo corresponds to the oil–water interface.

Therefore, the oil–water interface can be detected finding the location of maximum echo intensity. An example is shown in Fig. 10. To obtain the oil–water interface, the ultrasonic echoes at each profile were read in a Matlab code. The highest echo for each profile was detected and knowing that the channel distance was 0.74 mm, its distance from the surface was calculated. As such, the distance of the maximum echo from the UVP transducer for each profile was computed. The variation of these results over a certain time is representative for the variation of the oil–water interface in that time. Figure 10 shows the derived oil–water interface for a duration of 4.8 s. The period of 0.4 s (frequency of 2.5 Hz) seems to match the period of fluctuations appropriately. The values were smoothed with the moving average method in order to remove noise.

To obtain the velocity profile in oil and water, the interface position is detected during a certain time and the measured instantaneous velocity profiles are shifted to

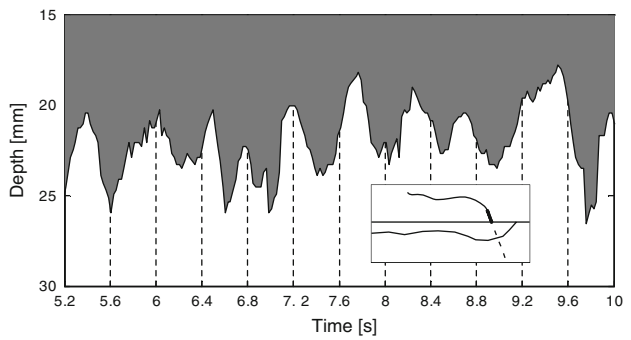

Fig. 10 Oil–water interface derived from echo intensity at frontward side of the slick headwave

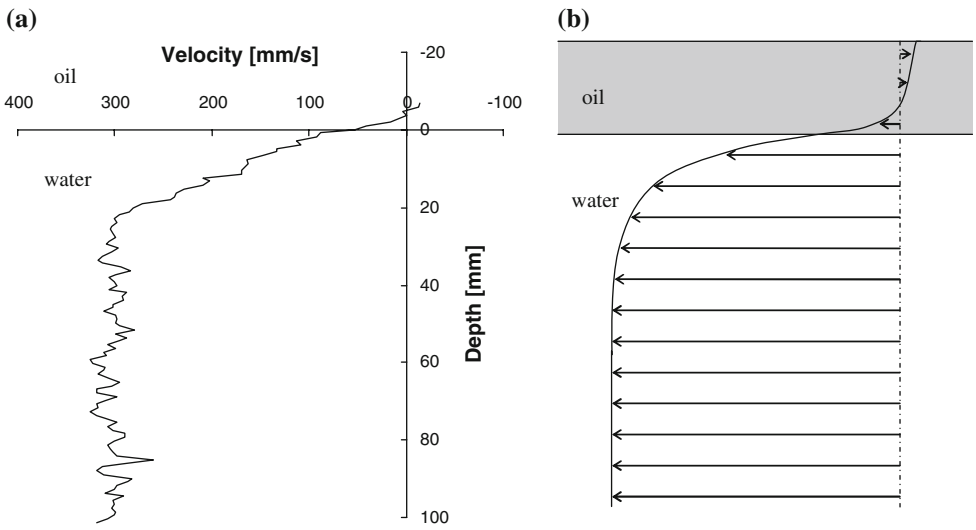

Fig. 11 Velocity profile in oil and water phases: **a** measured profile, averaged over 100 profiles, **b** representative velocity profile in two-phase oil–water fluid

achieve a constant interface position. The mean values of velocity in the oil and water phases are then calculated as seen in Fig. 11. It can be seen that a mutual coupling of the velocity field in water and oil gives a non-zero velocity at the oil–water interface. The flow is one directional in the water and bidirectional in oil. Schlichting and Gersten (1999) showed that, considering the dissipation, such a coupling is predictable in mixing layers. The velocity changes from almost zero to the ambient flow velocity in the water phase, i.e., a boundary layer develops close to oil–water interface. This can be justified since the water is less viscous than oil, and the energy dissipation is therefore smaller (Brouwers 2007; Zha 2004). Lee et al. (1991) determined the thickness of the water–oil interfacial roughness by means of neutron reflectivity study and showed that it is in the range of angstrom. Therefore, the interface is hydraulically smooth, and the velocity profile from oil to water is expected to change with a smooth curvature. This smooth velocity change was obtained in the present measurements as illustrated in Fig. 11a. As seen in this Figure, the velocity profile in the oil water interface has no discontinuity. Figure 11b illustrates a representative velocity profile in two-phase oil–water fluid with flowing water and contained oil layer.

6 Interfacial wave

The classical problem of Kelvin–Helmholtz (KH) instability is described in various textbooks (see, e.g. Chandrasekhar 1961; Drazin and Reid 2004). KH instability can occur when velocity shear is present within a continuous fluid or when there is sufficient velocity variation across the interface between two fluids. In general, instability occurs when there is some disturbance of the equilibrium of the external forces, inertia and viscous stresses in a fluid. Among the external forces of interest are buoyancy in fluids of different density, surface tension, magnetohydrodynamic forces. It was shown by Trallero et al. (1996) that the inviscid Kelvin–Helmholtz theory can be used to predict stratified flow with some mixing at the interface similar to the present case.

The waves traveling along the interface between two fluids whose dynamics are dominated by the effects of surface tension, known as capillary waves. The wavelength of these waves is defined as:

$$\lambda_c = \sqrt{\frac{\sigma}{g(\rho_w - \rho_o)}} \tag{5}$$

where σ is the oil–water interfacial tension. Leibovich (1976) and Delvigne (1991) attributed this same wave length to KH instabilities at oil–water interface.

Using the interfacial tension between water and rapeseed oil, 30 mN/m, in the Eq. 5, yields a value of 3.7 cm for the interfacial wavelengths. As seen in Fig. 8, the observed wavelength during the present experiments was about 4 cm which is in a good agreement with this capillary wavelength.

7 Conclusions

The velocity profiles and interfacial instability in a two-phase fluid were investigated. The velocity field was measured upstream of barriers of different types (rigid or flexible) and drafts. A first series of measurements was performed for water passing a barrier. The results showed that the type of the barrier does not influence the horizontal velocity field behind the barrier significantly in the far field. However, in the near barrier region, the barrier draft

and type changes the velocity field. The second series of measurements was taken for a situation in which an oil slick was contained behind the barrier. The results showed the effect of the oil layer on the velocity field to be more significant for barriers with deeper draft and at higher velocities.

The observed headwave at the upstream end of the oil slick was compared, in detail, to those of a gravity current. It was concluded that despite geometrical similarities, these two phenomena are quite different.

The capability of UVP measurements to detect the oil–water interface was confirmed and it could be shown that the location of maximum ultrasonic echo intensity accurately represented the interface. Using this, the velocity profiles in each phase were derived, showing that the boundary layer is located in the water, since it is less viscous and the energy dissipation is less in water.

Acknowledgments The research project is financed by the Swiss Petroleum Union under grant No. 4'09'02. The authors express their appreciation to Prof. Dr. Y. Takeda for his helpful comments on the measurements and data analysis, and to Met-Flow for providing technical support. The two anonymous reviewers are also greatly acknowledged for their detailed and useful comments.

References

Amini A (2007) Contractile floating barriers for confinement and recuperation of oil slicks. PhD thesis, No. 3941, Ecole Polytechnique Fédérale de Lausanne

Amini A, De Cesare G, Schleiss AJ (2006) Interface tracking and velocity profile in an oil–water two-phase flow. In: Fifth international symposium on ultrasonic Doppler methods for fluid mechanics and fluid engineering, ISUD 5, Switzerland, pp 125–128

Amini A, Kantoush SA, Schleiss AJ (2008) Velocity field measurements in the vicinity of an oil spill barrier using LSPIV method. In: International conference on fluvial hydraulics, River Flow, Turkey (accepted)

Benjamin TB (1968) Gravity currents and related phenomena. J Fluid Mech 31:209–248

Britter RE, Simpson JE (1978) Experiments on dynamics of a gravity current head. J Fluid Mech 88(2):223–240

Brouwers JJH (2007) Dissipation equals production in the log layer of wall-induced turbulence. Phys Fluids 19(10)

Chandrasekhar S (1961) Hydrodynamics and hydromagnetic stability. Oxford

De Cesare G, Schleiss A (1999) Turbidity current monitoring in a physical model flume using ultrasonic doppler method. In: Second international symposium on ultrasonic Doppler methods for fluid mechanics and fluid engineering, Switzerland, pp 61–64

Delvigne GAL (1991) On scale modeling of oil droplet formation from spilled oil. In: 12th international oil spill conference

Drazin PG, Reid WH (2004) Hydrodynamic stability, 2nd edn. Cambridge University Press, Cambridge

Fang F, Johnston AJ (2001) Oil containment by boom in waves and wind. III: Containment failure. J Waterway Port Coast Ocean Eng ASCE 127(4):234–239

Fannelop TK (1983) Loss rates and operational limits for booms used as oil barriers. Appl Ocean Res 5(2):80–92

Lee CM, Kang KH (1997) Prediction of oil boom performance in currents and waves. Spill Sci Technol Bull 4(4):257–266

Lee LT, Langevin D, Farnoux B (1991) Neutron reflectivity of an oil–water interface. Phys Rev Lett 67(19):2678–2681

Leibovich S (1976) Oil slick instability and entrainment failure of oil containment booms. J Fluids Eng Trans ASME 98(1):98–105

Lyons RG (2004) Understanding digital signal processing, 2nd edn. Prentice Halle PTR, Upper Saddle River

Met-Flow (2002) UVP-DUO User's guide, Release 5, Met-Flow SA, Lausanne, Switzerland

Milgram JH, Van Houten RJ (1978) Mechanics of a restrained layer of floating oil above a water current. J Hydronautics 12(3):93–108

Nakamura H, Kondo M, Kukita Y (1996) Simultaneous measurement of liquid velocity and interface profiles of horizontal duct wavy flow by ultrasonic velocity profile meter. In: First international symposium on ultrasonic Doppler methods for fluid mechanics and fluid engineering, Villigen, Switzerland, pp 29–32

Nakamura H, Kondo M, Kukita Y (1998) Simultaneous measurement of liquid velocity and interface profiles of horizontal duct wavy flow by ultrasonic velocity profile meter. Nuclear Eng Des 184:339–348

Schlichting H, Gersten K (1999) Boundary layer theory. Springer, Heidelberg

Shin JO, Dalziel SB, Linden PF (2004) Gravity currents produced by lock exchange. J Fluid Mech 521:1–34

Simpson JE (1972) Effects of the lower boundary on the head of a gravity current. J Fluid Mech 53(4):759–768

Simpson JE (1997) Gravity Currents: in the Environment and the Laboratory, 2nd edn. Cambridge University Press, Cambridge

Simpson JE, Britter RE (1979) The dynamics of the head of a gravity current advancing over a horizontal surface. J Fluid Mech 94(3):477–495

Takeda Y (1995) Velocity profile measurement by ultrasonic doppler method. Exp Therm Fluid Sci 10(4):444–453

Trallero JL, Sarica C, Brill JP (1996) A study of oil–water flow patterns in horizontal pipes. In: SPE annual technical conference, Denver, USA, pp 363–375

Von Karman T (1940) The engineer grapples with nonlinear problems. Bull Am Math Soc 46:615–680

Wicks M (1969) Fluid dynamics of floating oil containment by mechanical barriers in the presence of water currents. In: Conference on prevention and control of oil spills, pp 55–106

Willemetz JC (1996) Influences of fixed and moving interfaces in the measurement of velocity profiles. In: First international symposium on ultrasonic Doppler methods for fluid mechanics and fluid engineering, Villigen, Switzerland, pp 63–66

Xu Q (1992) Density currents in shear flow- a two-fluid model. J Atmos Sci 49(6):511–524

Xu Q, Moncrieff MW (1994) density current circulation in shear flows. J Atmos Sci 51(3):434–446

Zha GC (2004) Boundary-layer loss mechanism and assessment of wall function for turbulence modeling. AIAA J 42(11):2387–2390